SURFACE AND INTERFACE ANALYSIS
Surf. Interface Anal. 2006; **38**: 229–233
DOI: 10.1002/sia.2224

Surface basicity of ceria-supported lanthana. Influence of the calcination temperature

S. Bernal,[1] G. Blanco,[1]* A. El Amarti,[2] G. Cifredo,[1] L. Fitian,[1,2] A. Galtayries,[3] J. Martín[4] and J. M. Pintado[1]

[1] Departamento de Ciencia de los Materiales Ingeniería Metalúrgica y Química Inorgánica, Facultad de Ciencias, Universidad de Cádiz, E-11510 Puerto Real, Spain
[2] Faculté de Sciences, Université Abdelmalek Essâadi, Tétouan, Morocco
[3] Ecole Nationale Supérieure de Chimie de Paris, Paris, France
[4] Departamento de Química Física, Facultad de Ciencias, Universidad de Cádiz, Spain

Received 1 July 2005; Revised 15 November 2005; Accepted 26 November 2005

The surface basicity of pure ceria is strongly enhanced by the presence of the supported La_2O_3, the effect being very much influenced by the calcination temperature. X-ray diffraction (XRD), Raman spectroscopy, and La $3d_{5/2}$ XPS data for the different samples show a progressive incorporation of La^{3+} into the ceria lattice as the calcination temperature is increased. This structural change is considered to be responsible for the modifications that occurred in the basicity of the lanthana-modified ceria samples as revealed by temperature-programmed desorption-mass spectrometry (TPD-MS) of pre-adsorbed CO_2. Copyright © 2006 John Wiley & Sons, Ltd.

KEYWORDS: ceria-supported lanthana; surface basicity; TPD-CO_2; XPS; XRD; Raman spectroscopy

INTRODUCTION

Materials exhibiting strong surface basicity are receiving increasing attention in catalysis literature.[1] The rare earth oxides are acknowledged to belong to this category.[2,3] Among them, the lanthanum sesquioxide, La_2O_3, is known to exhibit the strongest basic character in the series.[3–5] Lanthana, however, has a major drawback; it is highly active against atmospheric water and carbon dioxide.[2,6,7] As a result, when manipulated in the air, it rapidly undergoes profound chemical, structural, and textural modifications.[2] In terms of catalytic applications, this lack of stability makes pure lanthana a material with severe handling problems. On the contrary, ceria, though not so strong a base material,[3–5] shows a much higher stability in air.[2]

Accordingly, it seemed interesting to us, to explore the basicity of materials resulting from the surface modification of ceria with highly dispersed lanthana. A number of references in the literature have dealt with acid-base[4,5] properties of La–Ce mixed oxides, but no similar information is presently available on ceria-supported lanthana systems.

In this work, we report on the characterisation of a ceria-supported lanthana sample, with a La : Ce molar ratio of 18 : 82, (18%)La_2O_3/CeO_2. In accordance with earlier studies on supported rare earth sesquioxide systems,[2,8–10] this loading roughly corresponds to a monolayer of the sesquioxide dispersed on the ceria surface. In our study, special attention will be paid to the influence of the calcination temperature (773, 973, 1173 K) on the basicity of the resulting materials. XPS, X-ray diffraction (XRD), Raman spectroscopy, and temperature-programmed desorption-mass spectrometry (TPD-MS) of pre-adsorbed CO_2 were used as experimental techniques.

EXPERIMENTAL

Sample preparation

The ceria-supported lanthana sample, with a La : Ce molar ratio of 18 : 82, (18%)La_2O_3/CeO_2, was prepared by incipient wetness impregnation technique from 1M aqueous solution of $La(NO_3)_3 \cdot 6H_2O$ Alfa Aesar (99.9% pure). The high-surface area (162 $m^2\ g^{-1}$) cerium oxide, 99.0% pure, used as support was kindly supplied by Rhodia. After the impregnation treatment, the sample was dried overnight in an oven at 383 K. Six cycles were required to achieve the required lanthana loading. The samples were finally calcined for 2 h at either 773, 973, or 1173 K. The resulting samples will be hereafter referred to as (18%)La_2O_3/CeO_2-500, (18%)La_2O_3/CeO_2-700, and (18%)La_2O_3/CeO_2-900, respectively. The chemical composition of the resulting material was confirmed by inductively coupled plasma (ICP) analysis. For comparative purposes, the starting high-surface area ceria was also calcined at the three temperatures mentioned above. In this way, CeO_2-500, CeO_2-700, and CeO_2-900 samples could be obtained.

---

*Correspondence to: G. Blanco, Departamento de Ciencia de los Materiales Ingeniería Metalúrgica y Química Inorgánica, Facultad de Ciencias, Universidad de Cádiz, E-11510 Puerto Real, Spain.
E-mail: ginesa.blanco@uca.es
Contract/grant sponsor: MCYT; Contract/grant numbers: MAT2002-02782; MAT2005-00333.
Contract/grant sponsor: *Junta de Andalucía* Group FQM-110; Contract/grant number: AM12/04.

Sample characterisation

The N_2 physisorption isotherms at 77 K were recorded on a Micromeritics, ASAP 2020, instrument.

The nature and concentration of base sites were studied by means of TPD-MS of pre-adsorbed CO_2. The experimental setup was coupled to a Pfeiffer, Thermostar GSD 301 T1 quadrupole mass spectrometer. The TPD-MS diagrams were recorded under the following conditions: He flow rate: 60 ml min^{-1}; heating rate: 10 K min^{-1}, amount of oxide sample: 100 mg. Prior to the TPD-MS runs, the samples were cleaned under 60 ml min^{-1} of 5% O_2/He, at 773 K (1 h); then, they were treated at 298 K, for 1 h, under 60 ml min^{-1} of pure CO_2 ($P_{CO_2} = 1$ atm), and finally flushed with He (60 ml min^{-1}), for 1 h, at 298 K.

The XPS data were recorded using a VG Escalab Mk II spectrometer, equipped with non-monochromatic Al Kα radiation. The powder samples were mounted on a double-sided adhesive conducting polymer tape, and analysed without any further treatment. Owing to the variable nature and amount of carbon-containing species in the samples, C 1s core level was not considered a reliable reference for binding energy correction. Instead, the higher binding energy peak of Ce3$\underline{d}$ core level, at 917.0 eV[11] was used as internal Ref. 12. The spectra were recorded in constant analyser energy (CAE) mode, using a pass energy (PE) of 20 eV for the detailed study of the different core levels of the samples. For the survey general spectra, the PE was increased to 100 eV.

XRD patterns were collected on a Bruker D8 Advance diffractometer, operating with Cu Kα radiation.

Raman spectra were recorded on an instrument consisting of a double monochromator Jobin Yvon, model U1000, a photomultiplier detector Hamamatsu, model R-943, and a Ar laser (514.5 nm) Spectra Physics, model 168.

RESULTS AND DISCUSSION

CO_2 chemisorption studies

Figure 1 and Table 1 summarise the results of the CO_2 chemisorption studies. The TPD-MS diagrams for CO_2 ($m/z = 44$) desorption from the series of ceria-supported lanthana and pure ceria samples are depicted in Fig. 1; whereas Table 1 accounts for the quantitative data for CO_2 desorption as determined by integration of the corresponding TPD-MS traces.

Regarding the results reported in Fig. 1 and Table 1, there are a number of aspects worth commenting on. First, the comparison of TPD diagrams depicted in Fig. 1(a) and (b) clearly show that the surface deposition of lanthana onto the ceria surface drastically modifies the desorption traces for CO_2. For pure ceria, the diagrams are dominated by a relatively weakly bound form peaking at temperatures slightly below 373 K. By contrast, the traces for (18%)La_2O_3/CeO_2 samples are spread over a much wider range of desorption temperatures with overlapping peaks at approximately 373, 573 and even above 773 K. We should conclude accordingly that the modification of ceria by lanthana induces the creation of much stronger base centres. Moreover, the total amount of desorbed CO_2 reported in the fourth column of Table 1 show that the modified ceria samples not only exhibit stronger basicity, but also a higher surface concentration of base centres.

The influence of the calcination temperature on both the surface concentration and strength of the base centres is also remarkable. As deduced from Table 1, the higher the

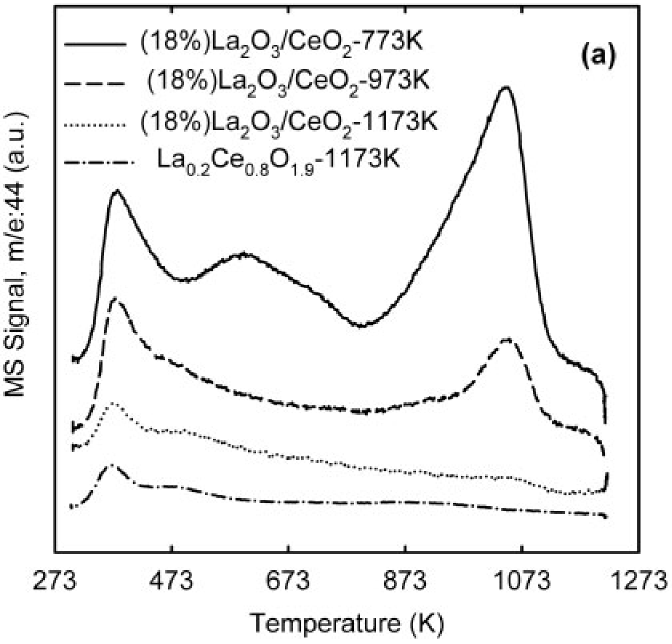

Figure 1. TPD-MS study of CO_2 ($m/z = 44$) desorption from the series of La_2O_3(18%)/CeO_2 (a) and pure CeO_2 (b) samples calcined at 773, 973 or 1173 K. For comparison, the trace for $La_{0.20}Ce_{0.80}O_{1.90}$-1173 K has also been included in Part (a) of the figure. Prior to the TPD runs, all the samples were heated under flowing 5% O_2/He, at 773 K (1 h), then they were treated with flowing CO_2 ($P_{CO_2} = 1$ atm), at 298 K (1 h), and finally flushed with He at 298 K (1 h). TPD experimental conditions: amount of sample: 100 mg; He flow: 60 cm^3 min^{-1}, heating rate: 10 K min^{-1}.

Table 1. Amounts of chemisorbed CO_2 as determined by integration of the corresponding TPD-MS diagrams

Sample–calcination temperature (K)	S_{BET} ($m^2\,g^{-1}$)	Total amount of desorbed CO_2[a] (mg of $CO_2\,g^{-1}$)	Total amount of desorbed CO_2[a] (molec nm^{-2})	Strongly chemisorbed CO_2[b] (molec nm^{-2})	Difference between data in columns no. 4 and no. 5 (molec nm^{-2})
CeO_2-773	139	9.1	0.9	0.3	0.7
CeO_2-973	43	3.5	1.1	–	–
CeO_2-1173	6	0.4	0.8	0.0	0.8
(18%)La_2O_3/CeO_2-773	49	26.4	7.4	4.3	3.1
(18%)La_2O_3/CeO_2-973	37	12.0	4.4	2.2	2.2
(18%)La_2O_3/CeO_2-1173	12	2.9	3.3	1.4	1.9
$La_{0.20}Ce_{0.80}O_{1.90}$-1173	10	2.5	3.5	1.9	1.6

[a] As determined from the TPD-MS traces recorded for the samples submitted to the cleaning routine and further treated with flowing CO_2 ($P_{CO_2} = 1$ atm), at 298 K (1 h).

[b] As determined from the TPD-MS traces recorded for the samples resulting from the cleaning routine with no further CO_2 treatment.

calcination temperature the lower the surface concentration of chemisorbed CO_2. Likewise, TPD diagrams, particularly those reported in Fig. 1(a), clearly show a progressive modification of the traces with preferential disappearance of the high-temperature peaks.

In accordance with the temperature applied during the 5% O_2/He pre-treatment of the samples, 773 K, the strongest forms of chemisorbed CO_2 might well not be completely eliminated by the cleaning routine. This means that the CO_2 treatment preceding the TPD runs would be applied to samples whose basicity is actually modified by the presence of the strongly chemisorbed CO_2 forms. To evaluate the quantitative relevance of the latter forms, parallel TPD experiments were run on the samples submitted to the cleaning routine with no further CO_2 treatment. The integration of these diagrams (not shown), allowed us to estimate the quantitative data reported in the fifth column of Table 1. As deduced from them, the strongest chemisorbed forms represent a significant fraction of the total desorbed CO_2, particularly in the case of the lanthana-modified samples. Remarkably, the relative weight of the high-temperature forms decreases with the calcination temperature. These forms very probably correspond to the free lanthana dispersed on the surface of the ceria, thus suggesting that the amount of surface lanthana progressively diminish with the calcination temperature. In agreement with this proposal, the TPD diagrams for (18%)La_2O_3/CeO_2-1173 K and $La_{0.20}Ce_{0.80}O_{1.90}$-1173 K, in Fig. 1(a), look quite similar to each other.

Though much less important in relative terms, the high-temperature desorption forms are also observed in pure ceria. In this case, however, the most likely origin for them is the decomposition of carbonate species trapped in the bulk of the oxide during its preparation.[13]

To fully understand the observations commented on above, a number of additional characterisation studies were performed. They will be briefly commented on below.

Other characterisation studies

Figure 2 reports on the $La3d_{5/2}$ XPS data for (18%)La_2O_3/CeO_2 samples calcined at 773, 973, and 1173 K. Reference spectra for $La_{0.20}Ce_{0.80}O_{1.90}$-1173 K and pure lanthana are also included in Fig. 2. The most remarkable

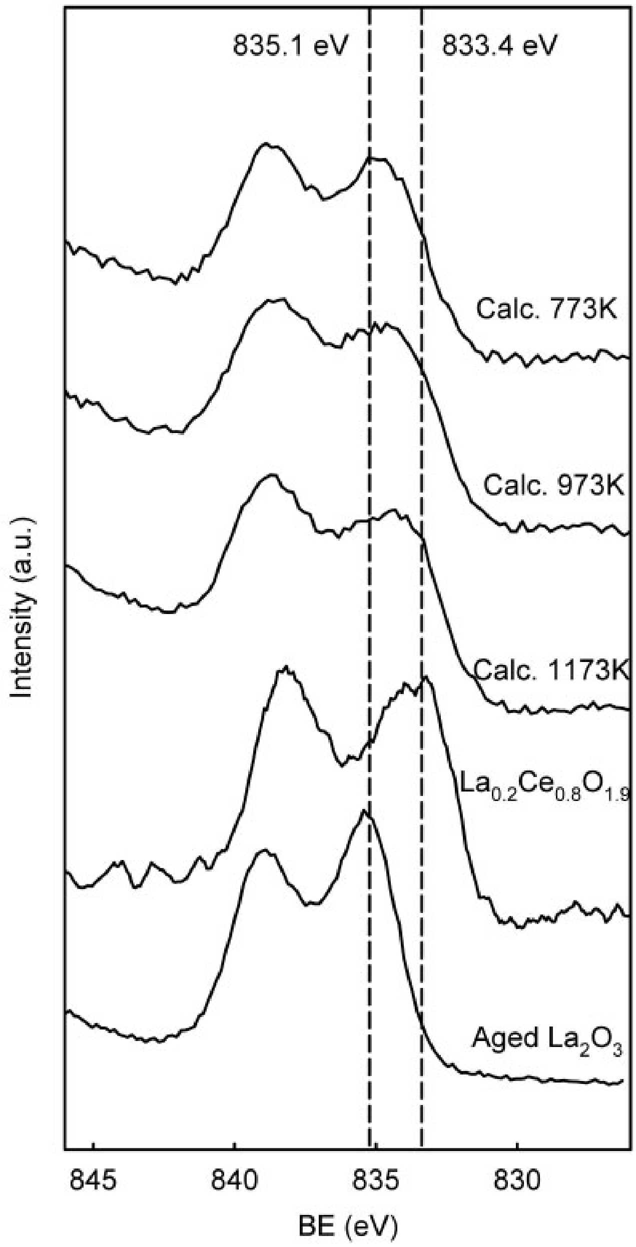

Figure 2. La $3d_{5/2}$ XPS spectra for (18%)La_2O_3/CeO_2 samples calcined at 773 K, 973 K, and 1173 K. Spectra corresponding to a Ce–La mixed oxide, $La_{0.20}Ce_{0.80}O_{1.90}$, and to a pure lanthana sample are also reported for comparison.

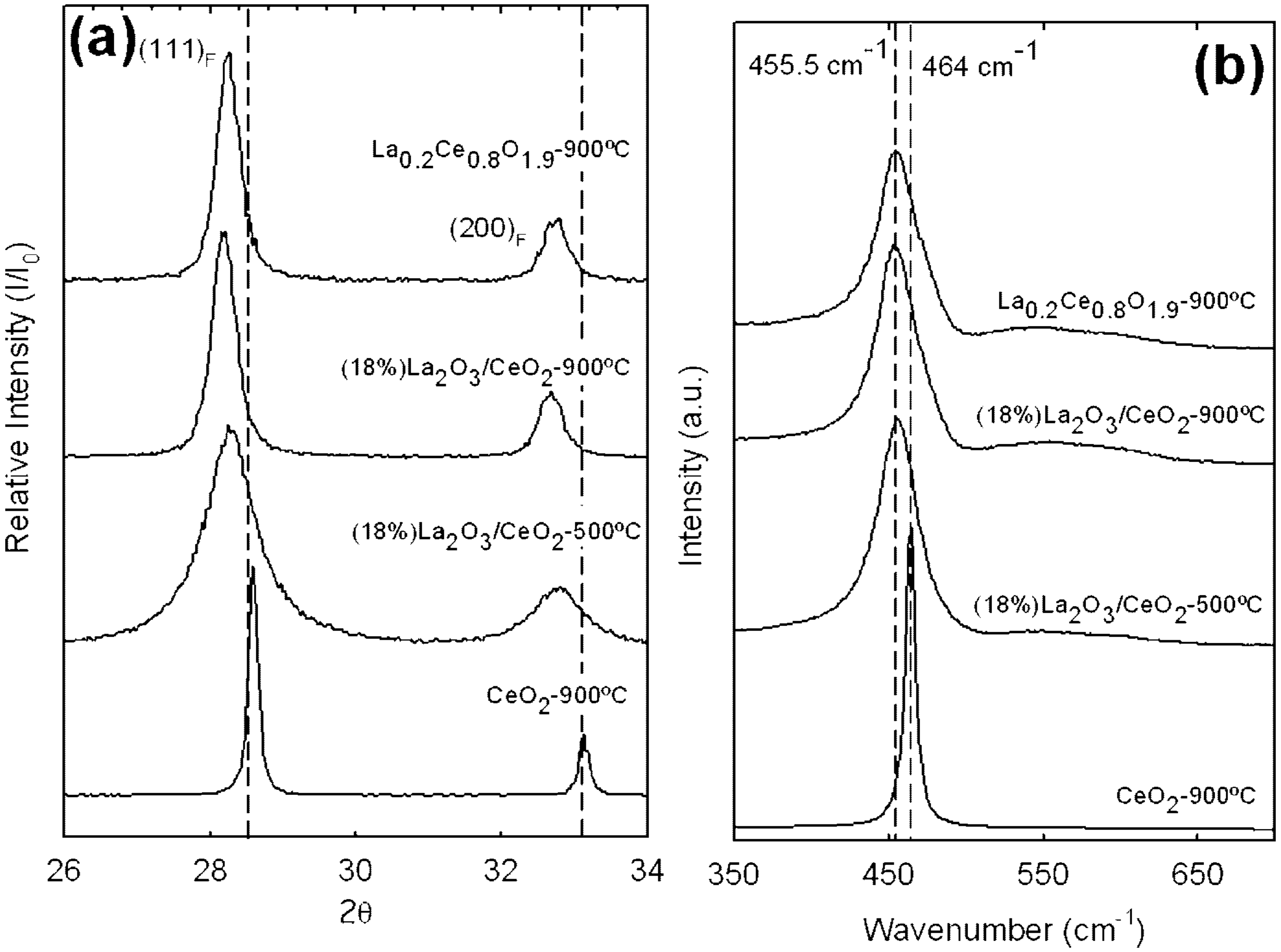

Figure 3. XRD (a) and Raman spectroscopy (b) studies of (18%)La_2O_3/CeO_2 samples calcined at 773 K and 1173 K. Diagrams for $La_{0.20}Ce_{0.80}O_{1.90}$ and CeO_2-1173 K are also included for comparison.

observation in the series of (18%)La_2O_3/CeO_2 sample spectra is the progressive development of a shoulder on the low-energy side of the peak at 835.1 eV. Though detectable in the (18%)La_2O_3/CeO_2-773 K sample, this shoulder, which is centred at 833.4 eV, is particularly noticeable in the sample calcined at 1173 K. As discussed in,[14] this effect may be interpreted as indicative of an evolution in the chemical environment of La^{3+} ions from a situation mainly consisting of free lanthana dispersed on the ceria surface, (18%)La_2O_3/CeO_2-773 K, to another one characterised by a majority of the La^{3+} incorporated into the fluorite lattice of the ceria support, (18%)La_2O_3/CeO_2-1173 K.

The XRD study is summarised in Fig. 3(a). In addition to the diagrams for (18%)La_2O_3/CeO_2-773 K and (18%)La_2O_3/CeO_2-1173 K, Fig. 3(a) includes those recorded for CeO_2-1173 K and $La_{0.20}Ce_{0.80}O_{1.90}$-1173 K. In the reported region of 2θ values (26°–34°), all the samples show two characteristic peaks of the fluorite structure. If the diagrams for pure ceria and the La–Ce mixed oxide are compared, a shift towards lower 2θ values may be observed in the latter. This shift, which indicates an increase in the lattice parameter of the mixed oxide with respect to that of CeO_2, is consistent with the incorporation of La^{3+} into the lattice of pure ceria. As in the case of the mixed oxide, the peaks observed in the diagrams for the supported lanthana samples appear shifted with respect to those for CeO_2. The effect is stronger for the sample calcined at 1173 K, whose diagram is very close to that of the mixed oxide. These observations are consistent with the occurrence of a progressive incorporation of La^{3+} ions into the ceria lattice as the calcination temperature is increased. The absence of any lanthanum-containing crystalline phase in the XRD diagrams for the La_2O_3/CeO_2 samples is also remarkable. This suggests that free lanthanum is present as either an amorphous and/or a highly dispersed phase.

The results of the Raman spectroscopy study are also in agreement with the observations above. As shown in Fig. 3(b), all the spectra exhibit the characteristic feature of the T_{2g} vibration mode in the fluorite structure.[15] However, it appears slightly shifted from 464.0 cm^{-1} in pure ceria, to 455.5 cm^{-1} in the mixed oxide, the bands for the ceria-supported samples peaking in between these two extreme values. In addition to this main feature, the spectra for the mixed oxide and the ceria-supported samples do also show a second, broader and much less intense band structure centred at approximately 570 cm^{-1}. As proposed in,[15,16] this peak may be attributed to the presence of O^{2-} vacancies in the lattice of the oxide. Therefore, its occurrence should also

DOI: 10.1002/sia

be considered as indicative of the La^{3+} incorporation into the ceria lattice.

CONCLUSIONS

The dispersion of lanthana on the ceria surface strongly modifies the basic behaviour of the support. This effect is particularly noticeable for the sample calcined at 773 K. As this temperature is increased, the contribution of high-temperature ($T_{desorption} > 773$ K) forms, i.e. of strongest basic centres, to the CO_2 desorption traces progressively decreases, that recorded for the sample calcined at 1173 K being similar to the one exhibited by $La_{0.20}Ce_{0.80}O_{1.90}$-1173 K. In agreement with the reported XPS, XRD, and Raman data, the evolution of the TPD-CO_2 diagrams with the calcination temperature is interpreted as being due to the progressive incorporation of La^{3+} ions into the ceria lattice, the strongest base centres being therefore associated with free lanthana highly dispersed on the ceria surface.

Acknowledgements

This work has been supported by the MCYT (Projects: MAT2002-02782 and MAT2005-00333) and the *Junta de Andalucía* (Group FQM-110, and Project: AM12/04).

REFERENCES

1. Kim HJ, Kang BS, Kim MJ, Park YM, Kim DK, Lee JS, Lee KY. *Catal. Today* 2004; **93–95**: 315.
2. Bernal S, Blanco G, Gatica JM, Pérez-Omil JA, Pintado JM, Vidal H. In *Binary Rare Earth Oxides*, Adachi G, Imanaka N, Kang Z (eds). Kluwer Academic Publishers: Amsterdam, 2004; 9, chap. 2.
3. Auroux A, Gervasini A. *J. Phys. Chem.* 1990; **94**: 6371.
4. Cutrufello MG, Ferino I, Monaci R, Rombi E, Solinas V. *Topics Catal.* 2002; **19**: 225.
5. Cutrufello MG, Ferino I, Monaci R, Rombi E, Colón G, Navío JA. *Phys. Chem. Chem. Phys.* 2001; **3**: 2928.
6. Rosynek MP. *Catal. Rev. – Sci. Eng.* 1977; **16**: 111.
7. Bernal S, Botana FJ, García R, Rodríguez-Izquierdo JM. *React. Solids* 1987; **4**: 23.
8. Yamamoto T, Tanaka T, Matsuyama T, Funabiki T, Yoshida S. *J. Phys. Chem. B* 2001; **105**: 1908.
9. Beguin B, Garbowski E, Primet M. *Appl. Catal.* 1991; **75**: **119**.
10. Bettman M, Chase RE, Otto K, Weber WH. *J. Catal.* 1989; **117**: 447.
11. Laachir A, Perrichon V, Badri A, Lamotte J, Catherine E, Lavalley JC, el Fallah J, Hilaire L, le Normand F, Quéméré E, Sauvion GN, Touret O. *J. Chem. Soc., Faraday Trans.* 1991; **87**: 1601.
12. Holgado JP, Alvarez R, Munuera G. *Appl. Surf. Sci.* 2000; **161**: 301.
13. Zotin FMZ, Tournayan L, Varloud J, Perrichon V, Frety R. *Appl. Catal.* 1993; **98**: 99.
14. Galtayries A, Blanco G, Cifredo GA, Finol D, Gatica JM, Pintado JM, Vidal H, Sporken R, Bernal S. *Surf. Interface Anal.* 1999; **27**: 941.
15. Rossignol S, Gérard F, Mesnard D, Kappenstein C, Duprez D. *J. Mater. Chem.* 2003; **13**: 3017.
16. McBride JR, Hass KC, Poindexter BD, Weber WH. *J. Appl. Phys.* 1994; **76**: 2435.

DOI: 10.1002/sia